J Wood Sci (2010) 56:366–370
DOI 10.1007/s10086-010-1106-5

ORIGINAL ARTICLE

Nobuo Sobue · Ian Woodhead

Improvement of simple impedance tomography method in RF range for estimating moisture distribution in squared timbers

Received: October 2, 2009 / Accepted: January 8, 2010 / Published online: April 27, 2010

Abstract Improvement of the simple tomography method for estimating moisture distribution in squared timbers was conducted by using impedance measurement in the RF range at 250 kHz. The local impedance in the horizontal and vertical directions was measured during natural drying. An inverse procedure using a trial-and-error method was used to reconstitute the cross-sectional moisture distribution from the surface impedance measurement. Two essential corrections for the spatial heterogeneity of the electric field between electrodes and for the calculation error due to the algorithm of the trial-and-error method were introduced to improve the accuracy of the reconstitution of the moisture distribution. The reconstituted moisture distribution matched well that determined by the oven-dry method.

Key words Moisture distribution · Tomography method · Structural timber · Impedance measurement · RF range

Introduction

Many types of electronic moisture meters are used in the wood industry. However, these meters are not sufficient to detect the moisture gradient in structural timbers. A computer tomography method using X-rays has been studied for standing trees[1] and for square timbers.[2] Another method using neutron beam imaging has been studied for wood disks.[3] These techniques can reproduce the cross-sectional moisture distribution, but they are too expensive to introduce into the wood industry. The other tomography method using impedance measurement has been studied in the high-frequency range[4–8] and using direct current.[9] From the point of view of improvement of the conventional electronic meter, a pin-type sensing probe with multiple hollow electrodes indenting in a specimen has been designed for measuring the moisture gradient at different depths.[10] Our final target is application of the impedance tomography technique in the radio frequency range to the inline grading of structural timbers with a low-cost moisture meter.

A recent study[4] showed potential for estimating the cross-sectional moisture distribution in structural timber by using the impedance tomography method. However, the reconstitution of the moisture distribution was not adequate for practical commercial use. This work aims to improve the reconstitution of moisture distribution by considering two kinds of signal correction. One corrects for the effect of the heterogeneity of the electric field between the electrodes and the other corrects for the flattening of the peak of the distribution pattern due to the inverse calculation algorithm used.

N. Sobue (✉)
Faculty of Agriculture, Shizuoka University, 836 Ohya, Suruga-ku, Shizuoka 422-8529, Japan
Tel. +81-54-238-4855; Fax +81-54-237-3028
e-mail: afnsobu@agr.shizuoka.ac.jp

I. Woodhead
Lincoln Venture Ltd., Lincoln, Christchurch 7640, New Zealand

Theory

Reconstitution of moisture content distribution

The algorithm used for the inverse calculation is commonly used for inverse problems in acoustic tomography and has the benefit of simple calculation but with limited resolution.[11] In this article, the moisture distribution was determined so that the moisture content of individual cells in Fig. 1 satisfy Eq. 1 using the simple trial-and-error method. Figure 1 shows the cross data table of 6×6 elements used to obtain the inverse solution. The value in each cell u_{ij} is the local moisture content. $U_{\mathrm{H}j}$ and $U_{\mathrm{V}i}$ are accumulated moisture contents of the rows and the columns, respectively:

$$U_{\mathrm{H}i} = \sum_{j=1}^{6} u_{ij} \quad \text{and} \quad U_{\mathrm{V}j} = \sum_{i=1}^{6} u_{ij} \tag{1}$$

The procedure for obtaining the solution is as follows:

In the first step, an average value of each accumulated moisture content, $U_{\mathrm{H}i}$, is distributed to each row cell:

u_{11}	u_{12}	u_{13}	u_{14}	u_{15}	u_{16}	U_{H1}
u_{21}	u_{22}	u_{23}	u_{24}	u_{25}	u_{26}	U_{H2}
u_{31}	u_{32}	u_{33}	u_{34}	u_{35}	u_{36}	U_{H3}
u_{41}	u_{42}	u_{43}	u_{44}	u_{45}	u_{46}	U_{H4}
u_{51}	u_{52}	u_{53}	u_{54}	u_{55}	u_{56}	U_{H5}
u_{61}	u_{62}	u_{63}	u_{64}	u_{65}	u_{66}	U_{H6}
U_{V1}	U_{V2}	U_{V3}	U_{V4}	U_{V5}	U_{V6}	

Fig. 1. Cross-sectional data table of 6 × 6 elements of moisture content distribution. U_{Hi} and U_{Vj} are the accumulated moisture contents in the row and column directions, respectively

$$u'_{ij} = U_{Hi}/6 \tag{2}$$

In the second step, the average of the difference of the accumulated moisture content in the column direction between U_{Vj} and the first estimated value is distributed to each row cell:

$$u''_{ij} = u'_{ij} + \left(U_{Vj} - \sum_{i=1}^{6} u'_{ij} \right) \Big/ 6 \tag{3}$$

This procedure is repeated in the row direction, and these two procedures are iterated until each value in the cross table converges to a stationary value. These series of inverse calculations were executed by an Excel (Microsoft) macro program.

Materials and methods

Boxed-heart squared green hemlock (*Tsuga heterophylla*) timber of 105 mm × 105 mm × 4 m was used. It was cut into twelve short specimens of 320 mm and both ends were sealed with silicone sealant. The specimens were dried under room conditions in the temperature range 13°–20°C and the average air dried density of the specimen was 490 kg/m^3. An impedance meter (Hioki-3531 Z HiTESTER) was used. The absolute value of the wood impedance Z was measured at 250 kHz with an excitation voltage of 1 V and the electrode arrangement shown in Fig. 2. The local impedance was measured by switching the detection electrode in turn from positions 1 to 6. A pair of thin polyethylene sheets was sandwiched between the electrodes and the timber. After the electrical measurement, the specimen was cut into 36 (6 × 6) pieces to determine the moisture content distribution by an oven-dry method.

Results and discussion

Fundamental equation converting impedance to moisture content

Past work[4] showed that the impedance measurement at 250 kHz is appropriate for the moisture measurement because the impedance change due to the moisture content change is stable and large at this frequency.

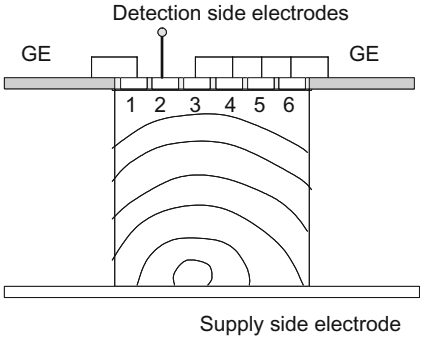

Fig. 2. Arrangement of the electrodes. *GE*, guard electrode

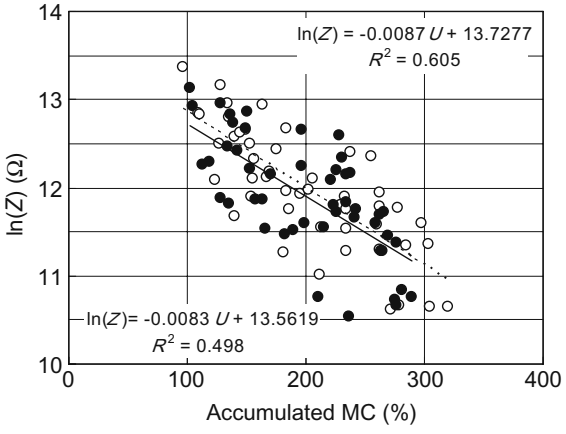

Fig. 3. Relationship between impedance ln(Z) and accumulated moisture content (MC) U of pooled data. *Open circles*, row direction; *solid circles*, column direction; R^2, coefficient of determination; *solid line*, column direction; *dashed line*, row direction

Figure 3 shows the relationship between the impedance and the accumulated moisture content in the directions of the 6 rows and 6 columns for the pooled data through all drying stages, where the accumulated moisture content is defined as the sum of moisture contents in each row or column direction. There was no significant difference between the regression equations for the row and column directions. Since these equations have acceptable correlation coefficients, the data in both row and column directions are pooled in the following analysis.

Corrections improving reconstitution of moisture distribution

It is well known and has been experimentally demonstrated that the temperature rise of timber piled between electrodes used for high-frequency drying of wood depends on the spatial position.[12] Hence the strength of the electric field between the electrodes shows a spatial heterogeneity.

Accordingly, prior to the reconstitution of the moisture distribution from the impedance data, the following two corrections were carried out: first, the correction for heterogeneity of the electric field in the cross section of the

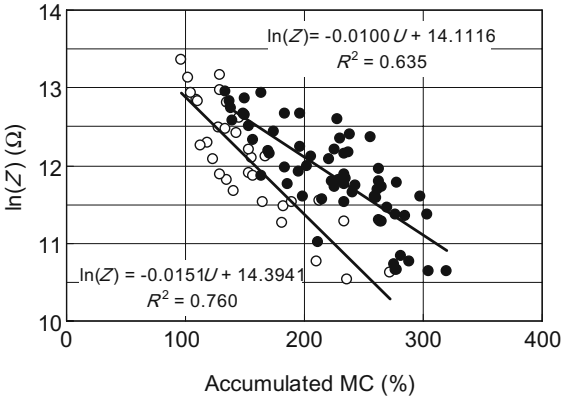

Fig. 4. Effect of spatial location in the relationship between impedance ln(Z) and U. *Solid circles*, core group; *open circles*, outer group

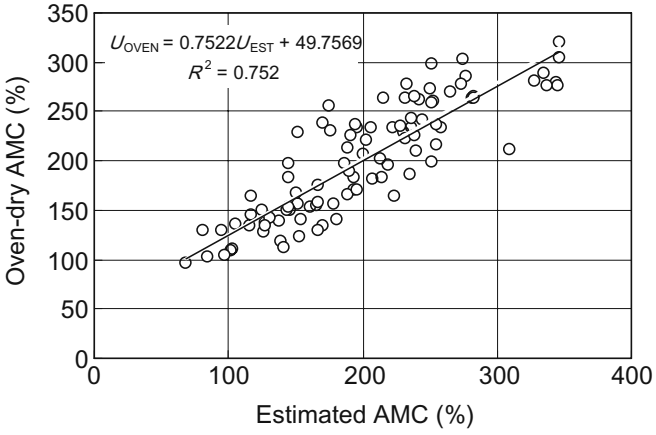

Fig. 5. Relationship between oven-dry accumulated moisture content U_{OVEN} and estimated accumulated moisture content U_{EST}. AMC, accumulated moisture content

material, and second, the correction for the inverse calculation.

Correction for heterogeneity of electric field

The first correction is to compensate for the field heterogeneity and it would depend on the spatial configuration of the electrodes, specimen size, and discontinuity of material properties. For the particular geometrical conditions of this experiment, the following two spatial groups were considered. One is made up of the outer rows and outer columns (U_{V1}, U_{V6}, U_{H1}, and U_{H6} in Fig. 1), and the other is made up of the core rows and columns (U_{V2}–U_{V5} and U_{H2}–U_{H5} in Fig. 1). The impedance versus moisture relationships were obtained for these two distinct groups.

Figure 4 shows the relationship between the impedance Z and the accumulated moisture content U. The regression lines for the core group and outer group are as follows:

$$\text{Core group: } \ln(Z_{core}) = -0.0100U + 14.112 \quad R^2 = 0.635 \quad (4)$$

$$\text{Outer group: } \ln(Z_{out}) = -0.0151U + 14.394 \quad R^2 = 0.760 \quad (5)$$

where R^2 is the coefficient of determination. The correlation coefficients were improved over those in Fig. 3 by separating the data into the two groups.

The estimated values of the accumulated moisture content Z_{EST} in the core and outer parts are given by the following equations inversely from Eqs. 4 and 5, respectively:

$$U_{ESTcore} = 1411.2 - 100\ln(Z_{core}) \quad (6)$$

$$U_{ESTout} = 953.2 - 66.23\ln(Z_{out}) \quad (7)$$

Figure 5 shows the relationship between the estimated accumulated moisture content U_{EST} for both row and column directions and the oven-dry accumulated moisture content U_{OVEN}, and the regression equation is given by:

$$U_{OVEN} = 0.7522U_{EST} + 49.757 \quad R^2 = 0.752 \quad (8)$$

Although the equation fits the data reasonably well (R^2 = 0.752), the predicted moisture content is under-estimated when below 200% and over-estimated when above 200%. In order to correct this trend, the combination of the Eqs. 6–8 was altered as follows:

$$U'_{ESTcore} = 1111.3 - 75.22\ln(Z_{core}) \quad R^2 = 0.7523 \quad (9)$$

$$U'_{ESTout} = 766.8 - 49.81\ln(Z_{out}) \quad R^2 = 0.7523 \quad (10)$$

This treatment, while unorthodox for linear regression, addressed the nonlinearity inherent in the electric field distribution. The resulting relationship between the modified moisture content and the oven-dry moisture content was given by:

$$U_{OVEN} = U_{EST} - 0.0015 \quad R^2 = 0.7523 \quad (11)$$

The gradient of the regression line became 1, and there was no difference in the coefficient of determination from Eq. 8.

Correction for algorithm in inverse calculation

The second correction in the inverse calculation was also a development beyond the previous work,[4] where the iterative method used was apt to flatten the peak of the resolved distribution. The effect was quantitatively evaluated using the original data set obtained from the cross-sectional distribution of the oven-dry moisture content. The original oven-dry moisture content data were compared with the reconstituted values to obtain the correction factors from eight data sets. The results were averaged and are shown in Fig. 6, which gives the magnitude of the correction factor applied to sharpen the moisture distribution. The correction factor in Fig. 6 shows that the uncorrected iteration method has a tendency to underestimate the core and four corner sections and to overestimate the remainder.

Application of two corrections to impedance data

The two corrections described above were adopted in the following order: first, the corrections for spatial position given by Eqs. 9 and 10 were applied and then the correction

for the inverse calculation procedure using the correction factor in Fig. 6 was adopted. Figure 7 shows the moisture content distributions for the oven-dry method and for the tomography method without corrections and after corrections. The prediction of moisture content distribution using the corrected inverse calculation showed a much closer alignment with the oven-dry results than those without the corrections.

Figure 8 shows the moisture content distribution for the oven-dry method and the reconstitution method. The relationship of the local moisture contents between the oven-dry method and the reconstitution method was given by the following equation:

$$u_{\mathrm{OVEN}} = 1.005u_{\mathrm{EST}} - 0.582 \quad R^2 = 0.713 \tag{12}$$

The deviation of Eq. 12 from the oven-dry results became large above the fiber saturation point, but since the main object of the application is the moisture inspection of structural timbers below the fiber saturation point, the obtained results are sufficient for practical evaluation of the moisture gradient of commercial timbers. The other important point is that the reconstituted cross-sectional moisture distribution gives us useful information to evaluate the drying process by determining whether the timber moisture content is within the target range to assure product quality. If a large moisture gradient remains in the timber, it may induce degradation such as checks and crooks during service. Figure 9 shows the relationship between the oven-dry average moisture content in the whole cross section and the predicted moisture content. The regression equation is as follows:

$$U_{\mathrm{whod}} = 0.8678U_{\mathrm{whest}} + 4.780 \quad R^2 = 0.780 \tag{13}$$

An alternative regression line with zero intercept is as follows:

$$U_{\mathrm{whod}} = 1.007U_{\mathrm{whest}} \quad R^2 = 0.759. \tag{14}$$

The average moisture content is also well estimated by this tomography method.

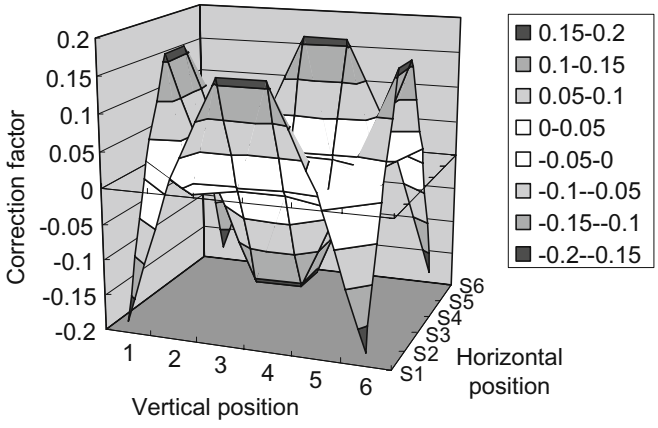

Fig. 6. Correction factor per unit moisture content applied prior to inverse calculation

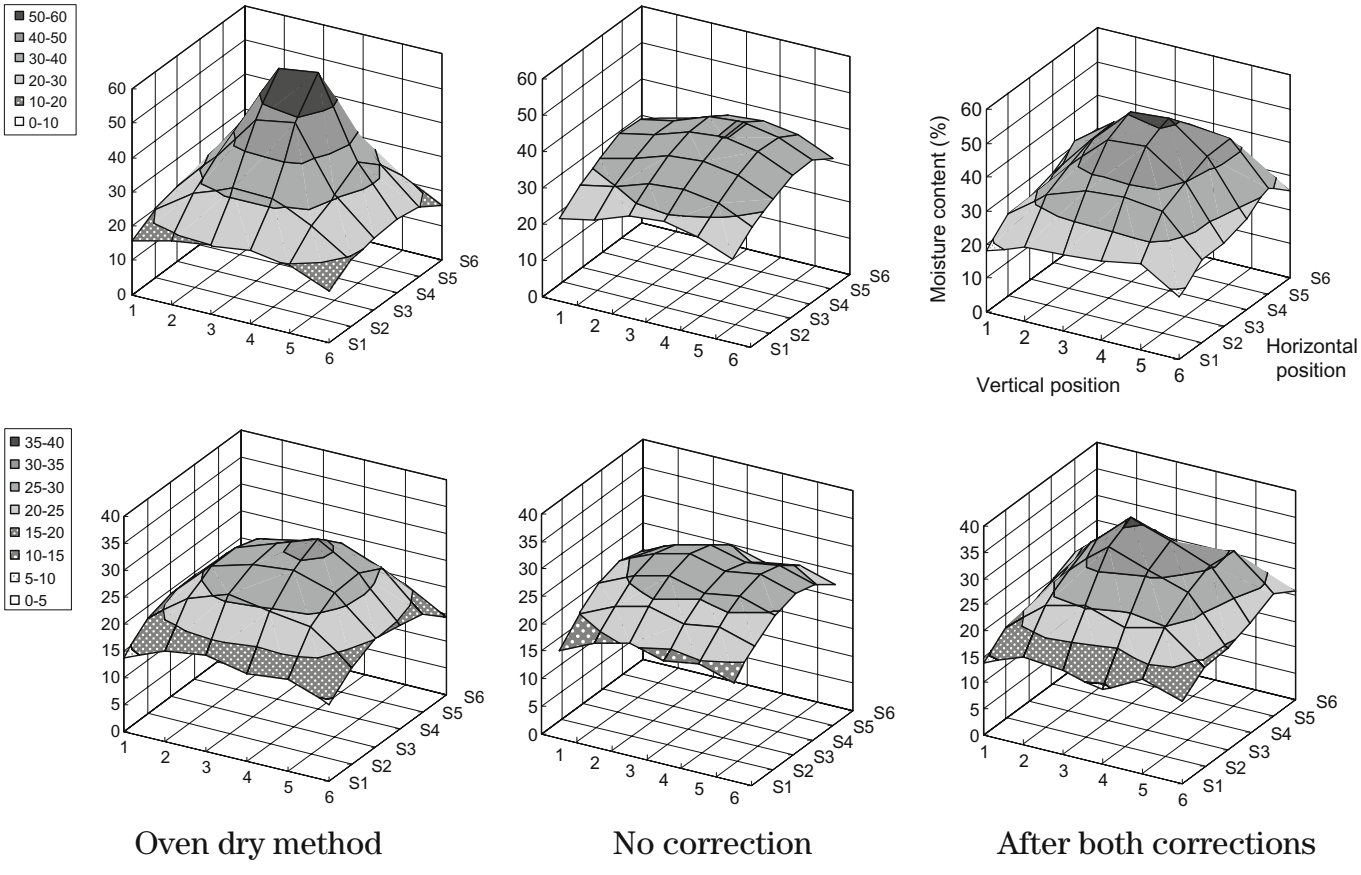

Fig. 7. Reconstituted moisture content (%) distributions. *Left*, oven-dry moisture content; *middle*, no correction; *right*, after both corrections

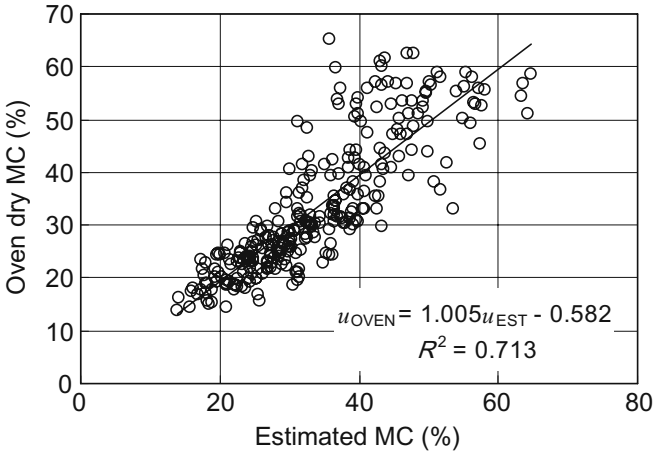

Fig. 8. Relationship between u_{OVEN} and u_{EST} for individual positions during all drying stages

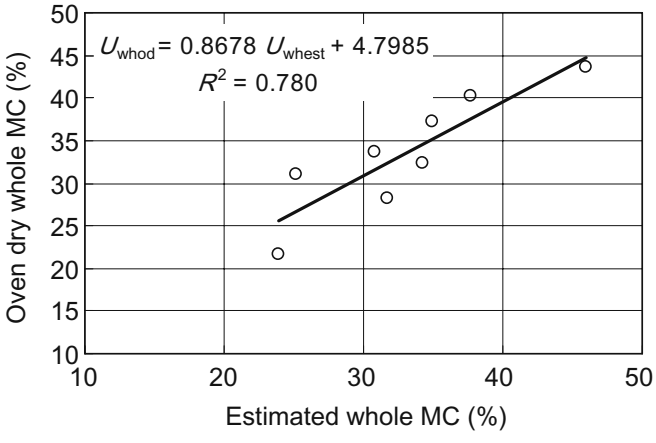

Fig. 9. Correlation of moisture content of whole specimen between the oven-dry method U_{whod} and estimation U_{whest}

Further improvement to the described method would require another calculation algorithm that takes account of the curvilinear nature of the electric force lines. Introduction of information on diagonal elements such as by using X-ray computer tomography methods could be used, but these are complex and expensive. The advantages of the impedance measurement are not only low equipment and processing costs, but also safety and ease of handling in the field and in the saw mill.

Conclusions

The proposed method aimed at improvement of the reconstitution of the moisture distribution in timber using impedance measurements. Corrections for the effects of the heterogeneity of the electric field and the inverse calculation algorithm were introduced. The results showed better reconstitution of the local moisture contents of commercial timbers than the previous approach did. This method is a key technique leading to realization of a moisture meter estimating the cross-sectional moisture distribution in commercial timbers.

Acknowledgment The authors wish to acknowledge Dr. Munehiro Date of the Kobayashi Institute of Physical Research for his advice on the design of the electrodes and discussions.

References

1. Kogure J, Kawamura H, Onoue M, Yamada H, Tsao JW (1984) Development of a portable X-ray computed tomographic scanner for measuring the annual rings of a live tree (in Japanese). Rigaku-Denki J 15:8–15
2. Kanagwa Y, Hattori Y (1985) Nondestructive measurement of moisture distribution in wood with a medical X-ray CT scanner II. Change in moisture distribution with drying (in Japanese). Mokuzai Gakkaishi 31:983–989
3. Nakanishi TM, Okano T, Karakama I, Ishihara T, Matsubayashi M (1998) Three-dimensional imaging of moisture in wood disk by neutron beam during drying process. Holzforschung 52:673–676
4. Sobue N, Inagaki M (2007) Estimation of cross-sectional moisture content in commercial timbers by impedance measurement in RF range. In: Proceedings of 7th International Conference on Electromagnetic Wave Interaction with Water and Moist Substances. Hamamatsu, Japan, April 15–18, pp 123–128
5. Suzuki Y (2007) Development of estimating method of moisture content of water distribution of Sugi (Japanese cedar) log using impedance measurements. In: Proceedings of 7th International Conference on Electromagnetic Wave Interaction with Water and Moist Substances. Hamamatsu, Japan, April 15–18, pp 107–113
6. Sobue N, Yokotsuka M (2003) Estimation of moisture gradient in timbers by capacity measurement in RF range with scanning electrodes. In: Proceedings of 5th International Conference on Electromagnetic Wave Interaction with Water and Moist Substances. Rotorua, New Zealand, March 23–26, pp 284–290
7. Titta M, Savolainen T, Lappalainen T (2003) Electrical impedance spectroscopy applications for wood moisture gradient measurement. In: Proceedings of 5th International Conference on Electromagnetic Wave Interaction with Water and Moist Substances. Rotorua, New Zealand, March 23–26, pp 277–283
8. Sobue N (2000) Measurement of moisture gradient in wood by electrode scanning moisture analysis ESMA. In: Proceedings of 12th International Symposium on Nondestructive Testing of Wood. Sopron, Hungary, September 13–15, pp 301–306
9. Sakai M, Hashimoto A (1998) Continuous measurement of moisture distribution in lumber. In: Proceedings of Annual Meeting of Chubu Branch of Japan Wood Research Society in 1998 (in Japanese). Toyama, Japan, August 27, pp 40–41
10. Forrer JB (1984) An electronic system for monitoring gradients of drying wood. Forest Prod J 34(7/8):34–38
11. Menke W (1989) Discrete inverse theory. Academic Press Inc., San Diego (Japanese translation by Yanagitani T, Tsukada K, Kokin Shoin, Tokyo, pp 198–202)
12. Terazawa S (1994) All about kiln drying of wood (in Japanese). Kaiseisha, Otsu, p 54, 116